Electron-Phonon Interaction in Single-Wall Carbon Nanotubes: A Time-Domain Study

Tobias Hertel and Gunnar Moos

Fritz-Haber-Institut der Max-Planck-Gesellschaft, Faradayweg 4-6, 14195 Berlin, Germany
(Received 30 November 1999)

We investigate the electron-phonon (e-ph) interaction in single-wall carbon nanotube samples at room temperature using femtosecond time-resolved photoemission. By probing electrons from the vicinity of the Fermi level we are able to study the e-ph interaction in the metallic nanotube species only. The observed electron dynamics can be used to calculate e-ph scattering matrix elements for two likely scattering scenarios: forward scattering from twistons and backscattering by longitudinal acoustic phonons. The corresponding matrix elements reveal an intrinsically weak e-ph interaction approximately 50% smaller than predicted by tight-binding calculations.

The electron-phonon (e-ph) interaction in carbon nanotubes gives rise to a variety of phenomena such as the temperature dependence of the electrical conductivity [1], the thermoelectric power [2], and possibly superconductivity [3]. Electron-phonon interactions can also induce subtle changes in the electronic band structure and open a small band gap at the Fermi level of metallic single-wall carbon nanotubes (SWNTs) [4,5]. Carbon nanotubes have furthermore been found to sustain very large current densities of 10^7–10^8 A/cm^2 at room temperature without suffering current induced damage [6,7], indicative of weak e-ph interactions that result in ballistic electron transport over long distances.

The strength of the e-ph interaction naturally plays a key role in these effects. However, a determination of the corresponding matrix elements from conventional transport studies, for example, is difficult due to the unknown residual resistivity, high contact resistances, the complex current path in SWNT samples of mixed tube types, etc. The intrinsic rate of energy transfer between electrons and lattice, however, should not be influenced by these effects. Here we present a direct measurement of the e-ph energy transfer in SWNTs at room temperature. This energy transfer can be obtained by studying the nonequilibrium electron dynamics after the system has been perturbed by rapid heating of the electrons with a femtosecond laser pulse [8]. By analyzing the dynamics of the electron distribution in the vicinity of the Fermi level we can determine the e-ph interaction in the metallic nanotube species. The resulting matrix elements are found to be considerably smaller than predicted by tight-binding calculations.

The sample preparation and experimental setup have been described elsewhere [9,10]. In short, the bucky-paper samples used in this study are produced from commercial SWNT suspension (tubes@rice, Houston, Texas) and contain a mixture of metallic and semiconducting SWNTs, in which the diameter distribution is sharply peaked at 12 Å [11]. Photoelectron spectra are obtained by means of the time-of-flight technique with an energy resolution of about 10 meV. The duration of the visible pump (typically 2.32 eV) and frequency doubled probe

pulses was 85 fs. The pump pulse fluence of typically 50 μJ/cm^2 is about an order of magnitude larger than the probe pulse fluence. For a review of the time-resolved photoemission technique, see Ref. [12]. To ensure reproducibility of the data, the experiments were performed at various spots on each of several different samples.

We start the discussion of our results with a calculation of the average density of states (DOS) of the bucky-paper samples. This is obtained by summing up the weighted DOS of all constituent nanotube types as determined by the diameter distribution given in Ref. [11] (we assume that chiral angles are distributed randomly). The DOS of the individual tubes is obtained from the electronic structure of graphene by zone folding its 2D band structure into the 1D Brillouin zone of the nanotubes [13]. The resulting average DOS for a nearest neighbor C-C hopping integral γ_0 of 2.6 eV is shown in the top panel of Fig. 1 together with the DOS of the $(9,9)$ nanotube—a highly probable metallic species within these samples. The spikes in the average DOS originate from the van Hove singularities of the various tube types. The cluster near ± 0.27 eV can be assigned to semiconducting nanotubes with an average band gap of about $0.22 \times \gamma_0 = 0.57$ eV. Between these spikes the average DOS is found to be constant since only metallic nanotubes contribute in this energy range. This becomes clearer in the middle panel of Fig. 1, where the DOS is plotted on an expanded energy scale. As discussed previously [9], spectral features in the bucky-paper DOS are broadened due to a combination of effects, such as the short lifetime of higher energy electrons and tube-tube interactions. In addition to this, the high sensitivity of photoelectron spectroscopy to the alignment of the band structure of individual tubes with respect to the vacuum level, in combination with possible impurity- or "self"-doping induced band shifts, leads to a further smearing of these structures in our spectra. Nevertheless, we expect the photoelectrons from the vicinity of the Fermi level to originate predominantly from metallic nanotubes.

The intensity of photoelectrons originating from the immediate vicinity of the Fermi level is primarily determined by the Fermi level DOS and the distribution function
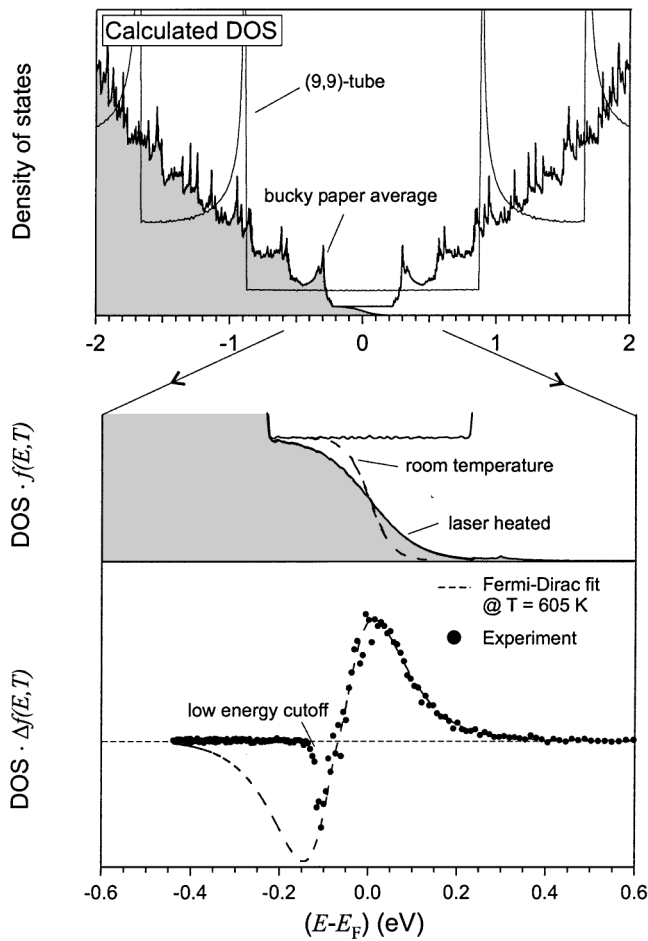
FIG. 1. Calculated average density of states of the bucky-paper samples (top panel). The density of states and laser induced changes in the distribution function near the Fermi level can be attributed to the dynamics in the metallic nanotube species of these samples (middle panel). The experimental photoelectron spectrum in the lower panel (correlated signal only) clearly shows the changes in the electron distribution due to heating of the electronic system.

$f(E, T)$, according to which the electronic states are occupied. This is also illustrated schematically in the middle panel of Fig. 1. In our time-resolved photoemission experiments a visible pump pulse initially generates a nonequilibrium electron distribution. The excited electrons rapidly lose energy by various scattering events until a new equilibrium at a somewhat higher electron temperature is established a few hundred femtoseconds later. This distribution can then be probed by a second UV laser pulse as a function of the time delay—similar to a pump-probe scheme previously applied to the electron thermalization in gold [14]. The lower panel of Fig. 1 shows an experimental photoemission spectrum, where—for clarity—we have plotted the difference between the newly equilibrated electron distribution and the unperturbed room temperature distribution. The energy of the probed electrons with respect to the Fermi level $(E - E_F)$ is calculated from the electron kinetic energy E_{kin} via the relation $(E - E_F) =$

$E_{kin} + e\Phi - h\nu_{probe}$, where $h\nu_{probe}$ is the probe photon energy and $e\Phi = 4.52 \pm 0.05$ eV is the sample work function. The trace in the lower panel of Fig. 1 clearly reveals that due to heating of the electronic system there is a depletion of the electron distribution below the Fermi level and an increase of the electron distribution above the Fermi level. A fit with a Fermi-Dirac (FD) distribution (dashed line) gives the best agreement for a fit temperature of 605 K (the pump-probe delay is 1.0 ps). We find no significant deviations from FD statistics near the Fermi edge. This justifies the use of FD statistics for the determination of the electron temperature despite the fact that *isolated* individual SWNTs should, in principle, observe Luttinger-liquid behavior typical for ideal one-dimensional systems [15]. We suggest that the absence of any obvious deviations from Luttinger-liquid-type behavior near the Fermi edge may either be due to tube-tube interactions or because such differences are too small to be observed with the present experimental setup. Deviations from FD statistics may become evident if these experiments were performed at very low temperatures—ideally on isolated individual nanotubes.

The evolution of the electron distribution at increasing pump-probe time delay is shown in Fig. 2 along with the best fit to a FD distribution. At zero pump-probe delay the electron distribution is not yet equilibrated and can only partially be described by a FD distribution. However, rapid scattering processes (most likely, electron-electron scattering) lead to thermalization within a characteristic time of about 200 fs which is estimated using the linear deviation of the measured signal from the FD fit. At 0.5 ps delay the deviation of the measured spectrum from the equilibrium FD distribution has become negligible. At longer time delays the temperature of the electron distribution continues
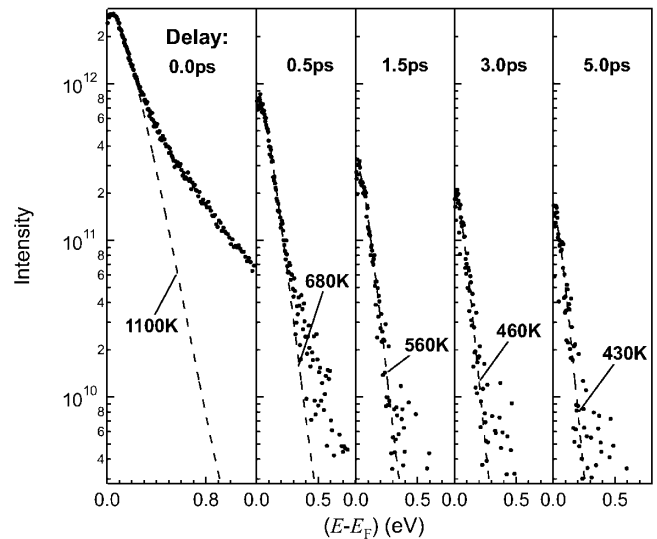

FIG. 2. Evolution of photoelectron spectra as a function of pump-probe delay. At pump-probe delays of over 200 fs, the spectra can be well described by a Fermi-Dirac distribution (dashed lines).

5003

to decrease towards the lattice temperature of 300 K. As expected for a metallic system—with a linear temperature dependence of the electron heat capacity—the peak temperature of the electron distribution was found to scale with the absorbed energy W as W^n with n ranging from $\frac{1}{2}$ to $\frac{1}{3}$.

The observed cooling of the laser heated electron gas is due to electron-phonon interactions and can be analyzed with respect to the contribution of different e-ph scattering processes. The nonequilibrium dynamics of an electronic system coupled to a phonon bath is frequently described in the framework of the two-temperature model [16]. Within this model, the evolution of electron and lattice temperatures T_e and T_1 is described by a set of coupled differential equations. Because of the morphology of the nanotube samples, we can neglect diffusive transport of charge carriers out of the excitation volume which reaches about 30 nm into the bulk material and is therefore comparable in size to typical nanotube rope diameters. The electronic heat capacity $c_e \approx 1.5$ mJ/(mol K) of metallic carbon nanotubes with typically 12 Å diameter is over 3 orders of magnitude smaller than the lattice heat capacity [17], so we can also neglect lattice heating. In this case the evolution of the electron gas temperature at the surface can simply be described by

$$C_e(T_e)\frac{\partial T_e}{\partial t} = -H(T_e, T_1), \qquad (1)$$

where $H(T_e, T_1)$ is the e-ph coupling term. This coupling term can be written as

$$H(T_e, T_1) = \sum_{q,k} \hbar\omega_q (W^e_{q,k} - W^a_{q,k}), \qquad (2)$$

where $W^e_{q,k}$ and $W^a_{q,k}$ are the transition rates for emission or absorption of a phonon by the electron in state k, respectively. The summation runs over all electron states k and phonon modes q. By using the tight-binding e-ph Hamiltonian given in Ref. [5] we obtain, from perturbation theory,

$$H(T_e, T_1) = \sum_q \int dE_k \frac{\pi N^2 \hbar \omega_q^2}{L} |g_{k;k+q}|^2 e^{E_k/k_B T_e}$$
$$\times (e^{\hbar\omega_q/k_B T_e} - e^{\hbar\omega_q/k_B T_1})n_q f(E_k)$$
$$\times f(E_k + \hbar\omega_q), \qquad (3)$$

where $N = \frac{L}{2\pi}\frac{2}{\gamma_0 a\sqrt{3}}$ is the nanotube density of states at the Fermi level, ω_q is the phonon energy, L is the tube length, and n and f are Bose and Fermi distributions, respectively. The e-ph matrix element $\sqrt{\frac{\hbar\omega_q}{2L}}\,g_{k;k+q}$ calculated by Jishi et al. [5] depends linearly on the term $q_0 = \frac{1}{\gamma_0}\left(\frac{\partial\gamma(\mathbf{r})}{\partial|\mathbf{r}|}\right)_0$ that gives the change of the nearest neighbor tight-binding matrix element as a function of the lattice distortion [18]. The cooling of the electronic system is then calculated from Eqs. (1) and (3) for forward scattering

by twistons (TW scattering scenario) and, alternatively, for backscattering from graphene derived longitudinal acoustic phonons (LA scattering scenario)—as this requires the use of different phonon dispersions in Eq. (3). These scattering processes are illustrated schematically in the inset of Fig. 3, where the nanotube band structure has been reduced to the two bands crossing the Fermi level. The phonon energies are obtained from the dispersion relations of the corresponding phonon modes of graphene with the sound velocities $v_{LA} = 20.35$ km/s and $v_{TW} = 9.42$ km/s [19]. Best agreement between the measured and calculated dynamics is obtained for $q_0 = 1.0$ Å^{-1} (TW scenario) and $q_0 = 0.8$ Å^{-1} (LA scenario) (see Fig. 3). The small systematic deviation of the calculated decay at longer time delays is likely due to strong excitation of the phonon modes with q close to 0 (TW scenario) or $q \cong -2k_F$ (LA scenario), i.e., a nonequilibrium phonon excitation.

The values for q_0 obtained from our experiment are considerably smaller than those derived by Pietronero et al. based on an estimate using the optical spectrum of polyacetylene ($q_0 = 2.0$ Å^{-1}) and tight-binding calculations for graphene ($q_0 = 2.5$ Å^{-1}) [18]. This difference is reduced somewhat if the appropriate overlap integral γ_0 of 2.6 eV is used instead of the too small value of 2.2 eV employed in Ref. [18]. Nevertheless, a discrepancy of nearly
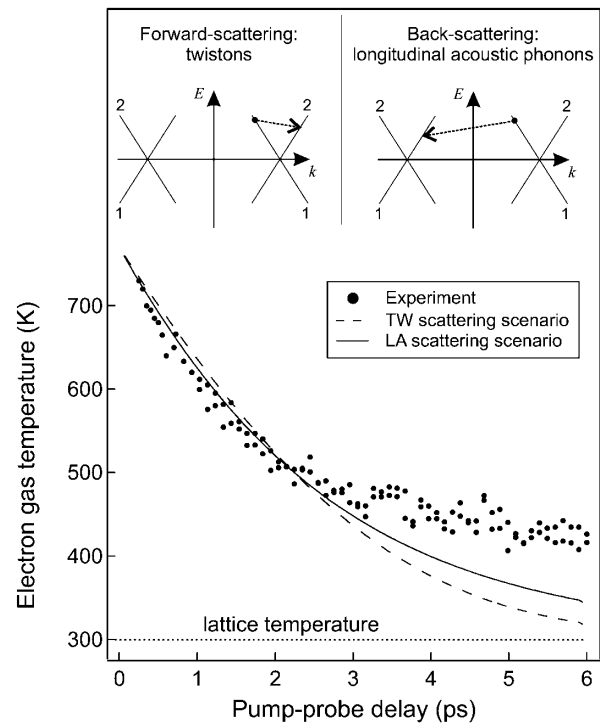

FIG. 3. Comparison of the measured cooling of the laser heated electronic system with calculations for two possible e-ph scattering scenarios. The inset shows a schematic illustration of the forward scattering by twistons and the backscattering by phonons derived from the longitudinal acoustic mode of graphene. The calculated cooling is plotted below for comparison with the experimental data.

50% between experimental and theoretical values remains. This gap even widens if the two scattering processes discussed above represent competitive channels for energy relaxation. This discrepancy may be indicative of partial "orbital relaxation"—an effect not accounted for by the tight-binding approach used in Ref. [18]—implying that orbitals do not rigidly follow the ions as they are displaced by a phonon.

By using reasonable values for q_0 and the matrix elements given in Ref. [5], we also find that backscattering from twistons is over 2 orders of magnitude too slow to give a significant contribution to the observed energy transfer rate. Scattering from other phonon modes such as transverse acoustic phonons and from optical buckling modes is, likewise, expected to be too weak to give a significant contribution to the e-lattice energy transfer rate [5,20].

In conclusion, we have determined the strength of the e-ph matrix element dominating the energy transfer between electrons and lattice in metallic SWNTs. Two different scattering scenarios give equally good agreement with the observed electron cooling rates: forward scattering by twistons and backscattering by phonons, derived from the longitudinal acoustic mode of graphene. Furthermore, a comparison with similar experiments on highly oriented pyrolytic graphite indicates an approximately twofold stronger e-ph interaction in SWNTs. By using Eq. (28) of Ref. [5] and the e-ph matrix element determined from experiment, the LA backscattering scenario yields a surprisingly high room temperature scattering time of almost 18 ps at the Fermi level. If we use a Fermi velocity of about 8 Å/fs this corresponds to a room temperature mean-free path of 14 μm which underlines the exceptional electronic transport properties of metallic SWNTs.

Such long mean-free paths may also contribute to the high stability of carbon nanotubes with respect to current induced damage.

[1] J. E. Fischer *et al.,* Phys. Rev. B **55**, R4921 (1997).
[2] J. Hone *et al.,* Phys. Rev. Lett. **80**, 1042 (1998).
[3] L. X. Benedict *et al.,* Phys. Rev. B **52**, 14 935 (1995).
[4] J. W. Mintmire *et al.,* Phys. Rev. Lett. **68**, 631 (1992).
[5] R. A. Jishi *et al.,* Phys. Rev. B **48**, 11 385 (1993).
[6] S. Frank *et al.,* Science **280**, 1744 (1998).
[7] Ph. Avouris *et al.,* Appl. Surf. Sci. **141**, 201 (1999).
[8] W. S. Fann *et al.,* Phys. Rev. Lett. **68**, 2834 (1992).
[9] T. Hertel and G. Moos, Chem. Phys. Lett. **320**, 359 (2000).
[10] E. Knoesel *et al.,* Phys. Rev. B **57**, 12 812 (1998).
[11] A. G. Rinzler *et al.,* Appl. Phys. A **67**, 29 (1998).
[12] S. Ogawa and H. Petek, Prog. Surf. Sci. **56**, 239 (1998).
[13] R. Saito, G. Dresselhaus, and M. Dresselhaus, *Physical Properties of Carbon Nanotubes* (Imperial College Press, London, 1998).
[14] W. S. Fann *et al.,* Phys. Rev. B **46**, 13 592 (1992).
[15] C. Kane *et al.,* Phys. Rev. Lett. **79**, 5086 (1997).
[16] M. I. Kaganov, I. M. Lifshitz, and L. V. Tanatarov, Sov. Phys. JETP **4**, 173 (1957).
[17] A. Mizel *et al.,* Phys. Rev. B **60**, 3264 (1999).
[18] L. Pietronero *et al.,* Phys. Rev. B **22**, 904 (1980).
[19] R. Saito *et al.,* Phys. Rev. B **57**, 4145 (1998).
[20] R. A. Jishi (private communication).